Transactions on Energy Systems and Engineering Applications

Article

Design and Cogging Torque Reduction of Radial Flux Brushless DC Motors with Varied Permanent Magnet Pole Shapes for Electric Vehicle Application

Tanuj Jhankal[1], and Amit N. Patel[1,*]

[1] Department of Electrical Engineering, Institute of Technology, Nirma University, Ahmedabad, India.
[*] Correspondence: amit.patel@nirmauni.ac.in

Received: 09 July 2023; Accepted: 26 August 2023; Published: 29 September 2023

Abstract: Brushless direct current motors have more attractive features, making them a promising solution for electric vehicle applications. A 1 kW, 510 rpm, 24-slots, and 8-pole inner runner type surface permanent magnet mounted radial flux brushless DC motor with seven different permanent magnet pole shape rotor is investigated in this paper. Motors with different permanent magnet shape rotors were designed and analyzed with finite element modelling and simulation. For performance comparison, the initial design with a radial-type pole shape was regarded as a reference design. In low-speed applications like electric vehicles, cogging torque is detrimental to the overall performance of the motor. The primary aim of this paper is to reduce the cogging torque, study its effect on the overall performance of the motor, and minimize torque ripples with reduced permanent magnet requirements. The proposed designs were analyzed in terms of cogging torque, flux density, torque, efficiency, flux linkage, and back-EMF. The comparative analysis shows that the motor with bump-shaped permanent magnet rotor poles outperforms the other designs.

1. Introduction

Electric vehicles (EV) are becoming increasingly well-liked due to the rising need for efficient and environmentally friendly transportation for reducing transportation-related carbon emissions [1–3]. The recent global energy crisis has also encouraged researchers to create "Eco-friendly" forms of transportation, such as fuel cells or battery-powered EVs with no emissions. However, the type of motor used substantially impacts these vehicles' overall performance [4]. Due to their high efficiency, low noise, high power density, high reliability, better dynamic response and compact design, permanent magnet (PM) brush-less direct current (BLDC) motors have emerged as a promising solution in this area [5, 6]. In comparison to conventional motors, BLDC motors use permanent magnets, which enhances the motor's performance as

How to cite this article: Jhankal, Tanuj; Patel, Amit N.. Design and Cogging Torque Reduction of Radial Flux Brushless DC Motors with Varied Permanent Magnet Pole Shapes for Electric Vehicle Application. *Transactions on Energy Systems and Engineering Applications*, 4(2): 535, 2023. DOI:10.32397/tesea.vol4.n2.535

the magnetic flux is generated without electric excitation and copper loss. The efficiency of BLDC motors is inherently better because of loss-free excitation from PMs. Various types of PMs are used in BLDC motors, like Ferrites, AlNiCo, Sm-Co (Samarium Cobalt) and NdFeB (Neodymium-Iron-Boron). NdFeB and Sm-Co are categorized as rare-earth magnets. With the highest energy product and considerably higher magnetic-flux production Neodymium-Iron-Boron is considered the best available magnet. Hence, it allows designing more compact motors than AlNiCo and ferrite magnets. Other advantages of using NdFeB are that it improves the dynamic response, enhances the steady-state performance, and improves the power density of the BLDC motors [7, 8].

Brushless direct current motors are classified into different types based on the magnetic flux arrangement and the permanent magnets' orientation. Three common classifications are radial flux BLDC (RF-BLDC), axial flux BLDC (AF-BLDC), and transverse flux BLDC (TF-BLDC) motors. Counter to the AF-BLDC motor and TF-BLDC motor, RF-BLDC motors have a simple structure, improved power transfer, reduced energy losses and allows faster acceleration & deceleration. However, it is essential to note that the selection of the most suitable motor type depends on the application's specific requirements. AF-BLDC and TF-BLDC motors have advantages and disadvantages, making them well-suited for specific applications. Therefore, it is essential to carefully evaluate the application's specific needs and consider each motor type's trade-offs and benefits before making a final decision.

Besides motor efficiency and size, torque quality is also a vital motor performance parameter. It is desired that a newly designed motor should produce the required torque with better quality. High torque ripple can significantly degrade the dynamic performance of an RF-BLDC motor by causing vibration and unwanted noise during motor operation. Reducing torque ripple is necessary for improving torque quality and overall performance. Cogging torque (CT), current harmonics, saturation of the magnetic circuit, and harmonics of the back-electromotive force (BEMF) are the causes that lead to the generation of torque ripple. Cogging torque is one of the significant reasons for torque ripple generation in RF-BLDC motors and is due to the interaction between permanent magnet magneto-motive force (MMF) and air-gap reluctance variation. Cogging torque does not play any role in producing the average torque (AT) of RF-BLDC motors. Instead, it contributes to the increment of torque ripple by superimposing with the AT profile of the motor. Torque ripple can be decreased by reducing cogging torque or by enhancing control circuitry/logic. Torque ripple is usually filtered out because of the moment of inertia of the system for high-speed applications, but at low-speed applications, torque ripple produces undesirable vibration and noise in the motor. Hence, to reduce the torque ripple and to improve the quality of motor torque, cogging torque needs to be minimized. There are methods of CT reduction in RF-BLDC motors either by motor design approaches or control approaches [9, 10]. The mitigation of the CT using motor design approaches is done by optimizing the motor's design parameters. In contrast, control approaches require precise current excitation and are highly dependent on the accuracy and reliability of the sensors used. Therefore, design-based approaches are more effective than control-based ones. Skewing of magnets or stator, slot opening variation, the addition of dummy slots, step skewing, unequal placement of rotor magnets, fractional of slots per pole, and segmented stator laminations are some techniques to minimize CT [11–15]. Skewing is widely adopted method in the industry [16]. Many researchers have been working in the CT reduction field using the techniques mentioned above. Some literature has proposed asymmetrical pole shaping technique [17] and the use of Herringbone design arrangement along with the conventional skewing method to overcome the unbalance in axial force [18].

This paper focuses on a comparative analysis of an inner runner type RF-BLDC motor with different magnet pole shape designs. It is preferable to maintain the same or lower magnet volume while using various PM shapes to accomplish the required outcomes. As most researchers attempt to reduce torque ripples while minimizing cogging torque and obtaining higher efficiency at a low expense of PMs, radial

pole shape variation in RF-BLDC motors can reduce cogging torque and thus improve the torque quality. By modifying the permanent magnet rotor pole (PM-RP) shape radially, different rotor configurations such as a center notched design, step-shaped, bread-loaf shaped, sinusoidal shaped, segmented pole, and bump shaped are implemented. A new bump-shaped rotor pole shape is presented to reduce the torque ripple, leading to the minimization of cogging torque with less permanent magnet material. The electromagnetic analysis was carried out on all the configured designs. According to this analysis, the proposed design RF-BLDC rotor with a bump-shaped permanent magnet pole has better electromagnetic performance regarding torque and cogging torque and the permanent magnet material requirement is also successfully reduced. The paper is structured as follows: Section 2 introduces the design of the RF-BLDC motor. A discussion of electromagnetic analysis parameters is presented in Section 3. In Section 4, the results of the analysis of all the designs are compared, while the conclusions are outlined in Section 5.

2. Design of RF-BLDC Motor

Figure 1 illustrates a 3-phase, 24-slot and 8-poles, 1 kW inner runner type surface permanent magnet RF-BLDC reference motor with radial PM-RP shape. Designing a surface permanent magnet (SPM) type RF-BLDC motor requires selecting several parameters, including slot-pole combination, material for core and permanent magnets pole, sizing constraints, winding type, magnetic and electrical loading and current density, and current density [19]. For designing a selected 1 kW rating motor, the current density is between 5-12 A/mm^2. For the construction of PM-RP, NdFeB (grade 38) material is used, and M19-29 grade non-oriented cold-rolled electrical steel material is used for the designing of stator teeth, rotor core and stator core. The main specifications of the initial design with radial magnet shape are listed in Table 1. Figure 2 presents the flowchart showing the complete design process with performance comparison of proposed PM-RP shapes. The shape and dimensions of the stator are kept the same for all designs. The dimensions of the rotor core are also kept the same for all designs, but the rotor configuration changes with each PM-RF shape, as shown in Figure 3. The motor's main parameters (i.e. length and diameter) remain unchanged, and lap-type winding is considered for all designs.

Table 1. Main design specifications of proposed 1 kW motor.

Parameters	Unit	Value
No. of phase	-	3
No. of poles	-	8
No. of slots	-	24
Stack length	mm	95.7
Stator outer radius	mm	81.5
Bore radius	mm	54
Air-gap length	mm	0.5
Slots/pole/phase	-	1
Fill factor	%	40
Permanent magnet height	mm	5
Magnet fraction	-	0.7
Permanent magnet remanence	T	1.2
Permanent magnet material	Grade - 38	NdFeB
Core material	Grade - 29	M19

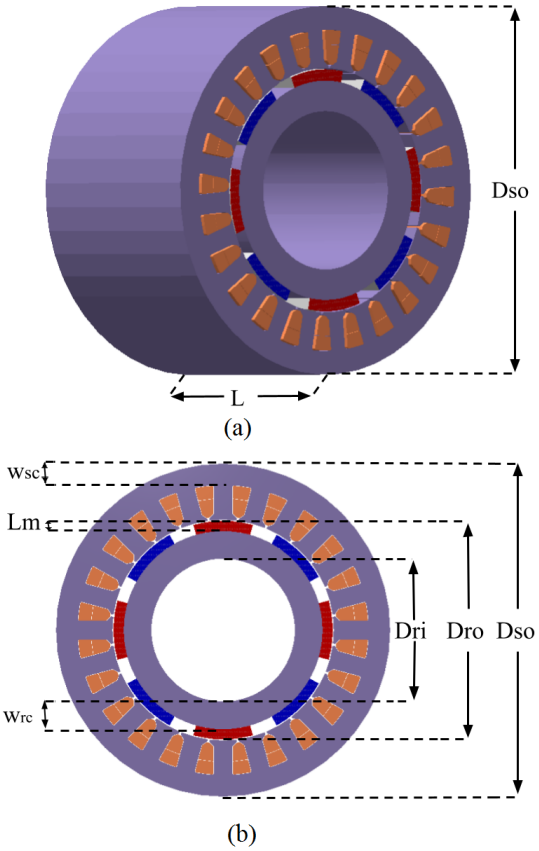

Figure 1. Constructional view of RF-BLDC motor with design parameters.

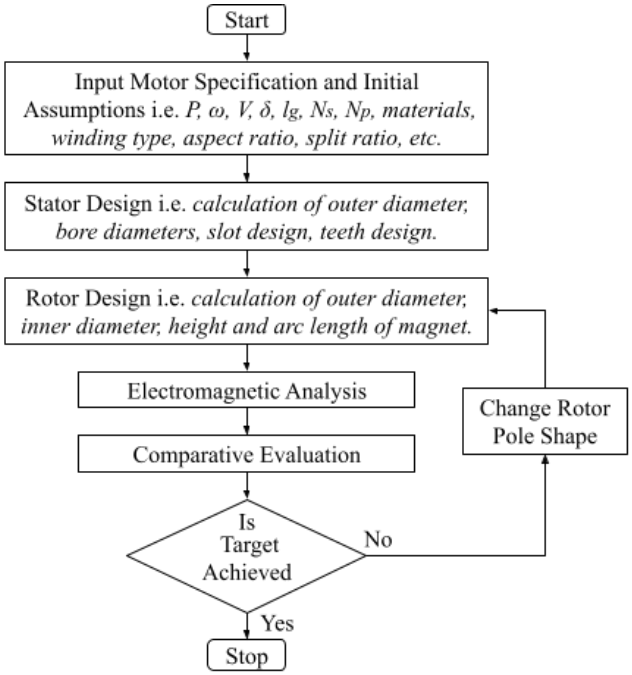

Figure 2. Flowchart for designing of RF-BLDC motor with different rotor pole shape topologies.

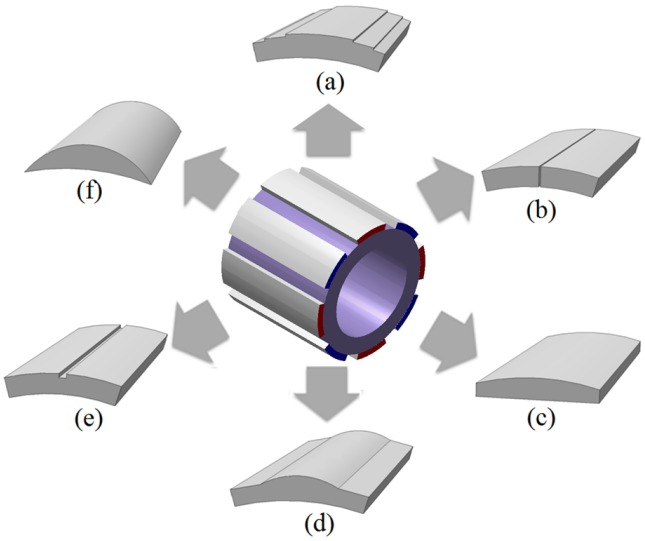

Figure 3. Rotor structure of RF-BLDC motor with various permanent magnet pole shapes: (a) step-shaped, (b) segmented, (c) bread-loaf shaped, (d) bump-shaped, (e) center notched, (f) sinusoidal-shaped, and radial shaped in center.

3. Electromagnetic Analysis

The electromagnetic analysis evaluated various performance parameters, including torque profile, cogging torque profile, flux density plot, flux linkage profile, efficiency, weight, and back-EMF. The flux density plot of 1 kW, 510 rpm RF-BLDC motor with different PM-RP shapes were obtained with finite element analysis. Figure 4 shows the flux density plot of the reference design, which has conventional radial-shaped magnet poles. Figure 5 features the step-shaped PM-RP design. Figure 6 presents the segmented PM-RP configuration. Figure 7 depicts the bread-loaf PM-RP design. In Figure 8, we observe the flux density plot for the bump-shaped PM-RP design, followed by Figure 9, which showcases the center notched PM-RP. Finally, Figure 10 illustrates the sinusoidal PM-RP design.

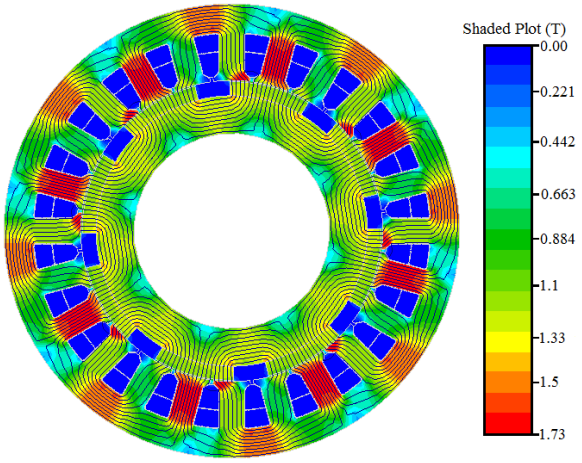

Figure 4. Flux density plot 1 kW reference model.

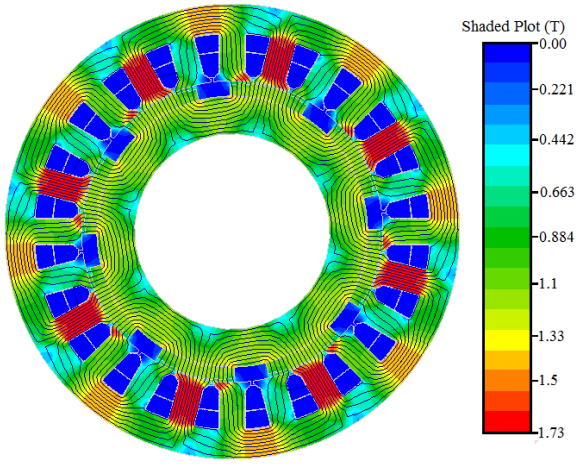

Figure 5. Flux density plot of 1 kW with step-shaped rotor pole.

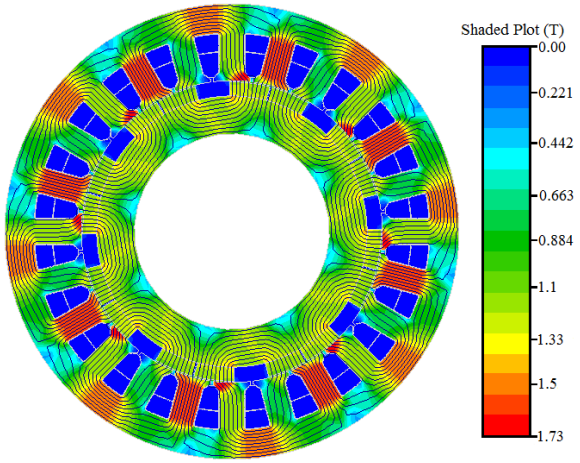

Figure 6. Flux density plot of 1 kW with segmented rotor pole.

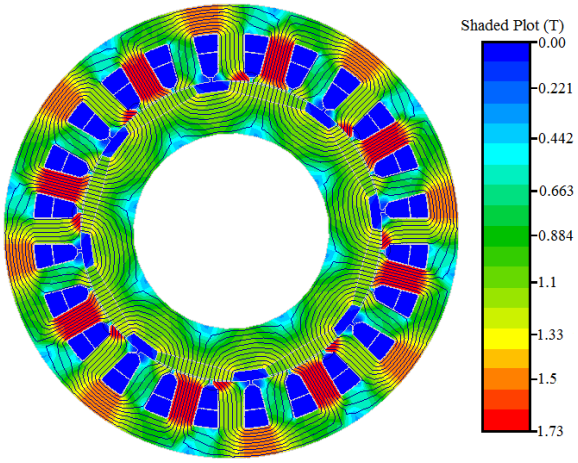

Figure 7. Flux density plot of 1 kW with bread-loaf shaped rotor pole.

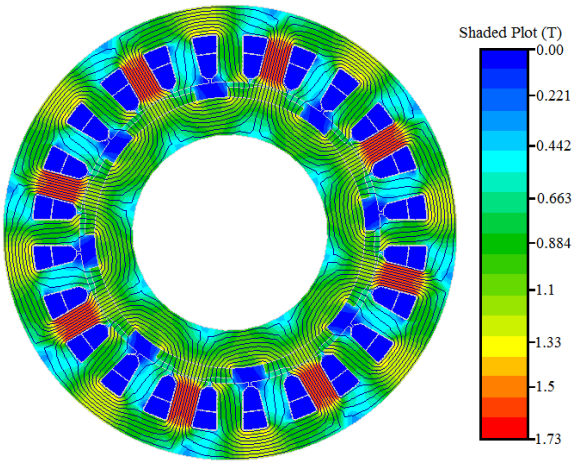

Figure 8. Flux density plot of 1 kW with bump-shaped rotor pole.

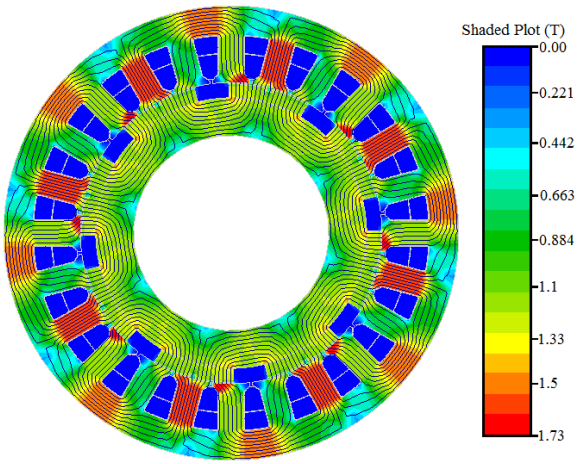

Figure 9. Flux density plot of 1 kW with center-notched rotor pole.

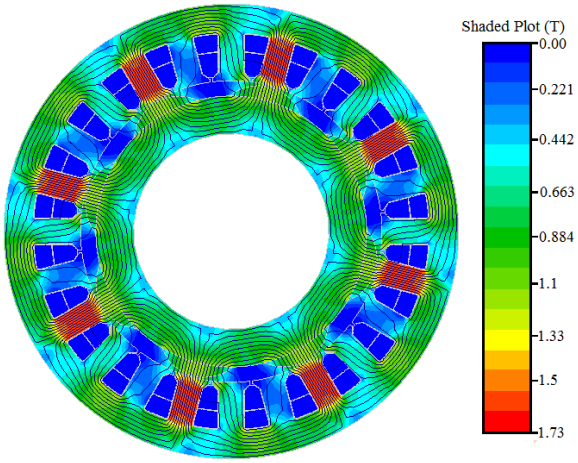

Figure 10. Flux density plot of 1 kW with sinusoidal rotor pole.

3.1. Cogging Torque

Cogging torque is one of the inherent characteristics of an RF-BLDC motor. It occurs due to the interaction between stator teeth and the rotor side permanent magnet poles of RF-PMBLDC motors. In RF-BLDC motors, the stator teeth are the reluctance variation source, whereas magnetic flux variation is majorly due to permanent magnet poles. Cogging torque is present even if no supply is provided to the stator windings (hence, it is also known as no-current torque) and has a periodic nature because of periodic air-gap reluctance variation. The cogging torque is expressed as [20–23]:

$$T_{cogg.} = -\frac{\partial W}{\partial \theta} \ , \tag{1}$$

where W represents the magnetic-field energy and θ is the rotor angle. For RF-BLDC motors, if we neglect the radial edge effects, then the expression for the stored magnetic-field energy can be written as,

$$W \cong W_{magnet+air-gap} \tag{2}$$

or

$$W = \frac{\int_V C_0 B_\alpha^2 (\beta)\, dV}{2\mu_0} \ , \tag{3}$$

where V is the volume of air-gap, β is the circumference angle of air-gap, $B_\alpha(\beta)$ is the distribution of the air-gap flux density, and μ_0 is the free space permeability. The air-gap relative permeance can be expressed as

$$C(\beta,\theta) = \left(\frac{h_m(\beta)}{h_m(\beta) + \delta(\beta,\theta)}\right)^2 \ , \tag{4}$$

where h_m is the length of the PM in the magnetization direction and $\delta(\beta,\theta)$ is the distribution function of effective air-gap length. The Fourier expansions of B_α^2 and C are

$$B_\alpha^2(\beta) = B_{\alpha\beta} + \sum_{j=1}^{\infty} B_{\alpha j} cos(2jp\beta) \tag{5}$$

and

$$C = C_0 + \sum_{j=1}^{\infty} C_j cos(jN_s(\beta+\theta)) \ . \tag{6}$$

where C_0 and C_j are the Fourier series coefficients and N_s is the number of slots. Rewriting Equation 1 by using Equations 2-6, $T_{cogg.}$ is expressed as,

$$T_{cogg.}(\theta) = \frac{\pi z \delta \left(R_o^2 - R_i^2\right)}{4\mu_0} \sum_{j=1}^{\infty} jC_j B_{\alpha \frac{jz}{2p}} sin(jz\theta) \tag{7}$$

where R_i is the inner radius of the RF-BLDC motor, R_o is the outer radius of the motor, p is the number of pole pairs, and z is the least common multiple of N_s and p. It can be seen in Equation 7 that the cogging torque is the sum of a series of torque harmonics and is directly affected by the change in the permanent magnet pole shape. Changes in the PM-RP shape affect the values of $B_\alpha(\beta)$ and $C(\beta,\theta)$. This results in the change in stored magnetic-field energy and finally affects cogging torque of the motor, as shown in Equation 7. Figure 11 compares cogging torque profile obtained from the electromagnetic analysis of the

reference and proposed PM-RP shape models. The model with a sinusoidal PM-RP shape has the lowest peak-to-peak cogging torque value compared to other designs.

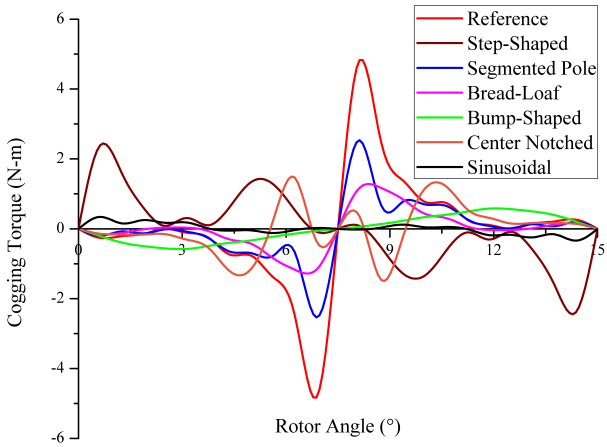

Figure 11. Cogging torque profile comparison of all the proposed and the reference RF-BLDC motor.

3.2. Average Torque

The average torque of a 3-phase, 24-slots/8-poles, 1 kW, 510 rpm motor is analyzed and investigated for all the designed models. The torque profile of all the models designed using the proposed PM-RP shapes are compared with the reference design in Figure 12. The average torque of the reference and the proposed PM-RP shapes models are investigated at a current density of 5-12 A/mm^2 The AT of the reference design having a conventional radial magnet shape is 18.90 N·m, whereas for the design with step-shaped PM-RP is 17.8 N·m, that of the segmented pole design is 18.70 N·m, for the design with bread-loaf shape is 19.1 N·m, that of the bump-shaped PM-RP design is 15.5 N·m, for center-notched design is 18.7 N·m and that of the sinusoidal PM-RP design is 13.4 N·m. The design with bread-loaf-shaped PM-RP gives the highest value of average torque. To assess torque ripple, the percentage was calculated as

$$T_{ripple}(\%) = \frac{T_{maximum} - T_{minimum}}{T_{average}} \times 100 \tag{8}$$

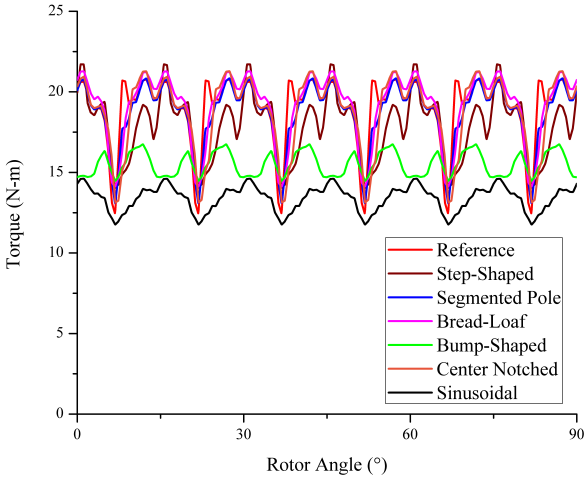

Figure 12. Torque profile comparison of all the proposed and the reference RF-BLDC motor.

3.3. Flux Linkage

This section presents the comparison of flux as a function of rotor angle, as shown in Figure 13. Figure 14 illustrates the amplitude comparison of different harmonic orders present in the flux linkage profile of all the designs. The total harmonic distortion (THD) of the flux linkage curve is also calculated for all the designs. The reference design exhibits a THD of 4.88%, while the other PM-RP shape designs, which are step-shaped, segmented pole, bread-loaf, bump-shaped, center-notched and sinusoidal, show THD values of 3.82%, 5.29%, 4.67%, 4.18%, 5.36%, and 10.09%, respectively. The THD in the sinusoidal-shaped PM-RP model increases as the value of the fundamental component decreases to 74.6 mWb, whereas the reference design maintains a value of 100 mWb, as shown in Figure 14. The designs with step-shaped PM-RP, bread-loaf-shaped PM-RP, and bump-shaped PM-RP show better performance with enhanced flux linkage.

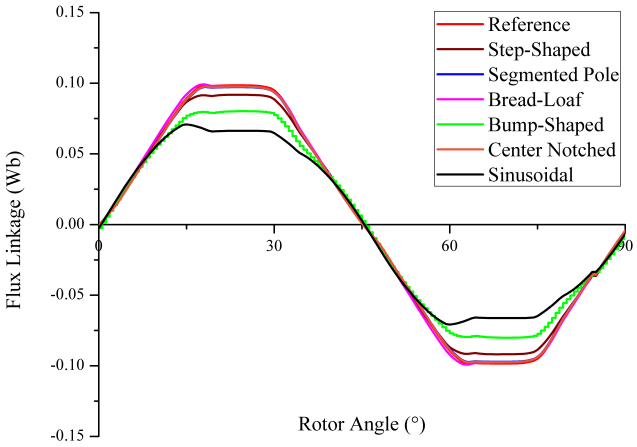

Figure 13. Flux linkage profile of all RF-BLDC motors with different PM-RP shapes.

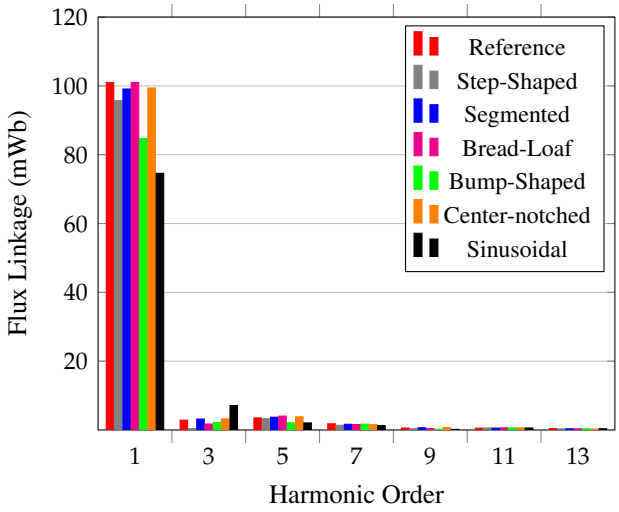

Figure 14. Flux linkage harmonic content amplitudes of all designs.

3.4. Back-EMF

Electromotive force is induced when the flux linkage in any coil changes. It can easily be expressed as the rate of change of flux with respect to time. In the case of the RF-BLDC motor, back-EMF is

directly related to the motor's torque. Figure 15 presents the back-EMF as a function of rotor angle for all designs. It is observed that the peak back-EMF value is reduced in the case of step-shaped PM-RP design, segmented-pole design, bump-shaped PM-RP design, and sinusoidal-shaped PM-RP design. A slight increment is also observed in the case of bread-loaf-shaped PM-RP and center-notched-shaped PM-RP models. Figure 16 shows the amplitude comparison of different harmonic orders in all the designs' back-EMF profiles. A higher THD value indicates more distortion in back-EMF, which can significantly affect the motor's efficiency, torque quality, and overall performance. This relationship is described by the equation

$$\mathrm{THD}(\%) = \frac{\sqrt{\sum_{j=2}^{n} Q_j^2}}{Q_1} \times 100, \tag{9}$$

where Q_j is the harmonic component present in the profile, Q_1 denotes the fundamental component, and j is the total number of harmonic components.

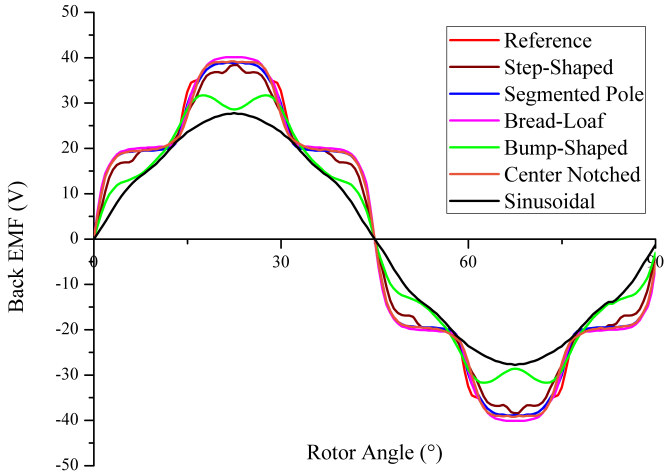

Figure 15. Back-EMF profile of all RF-BLDC motor with different PM-RP shapes.

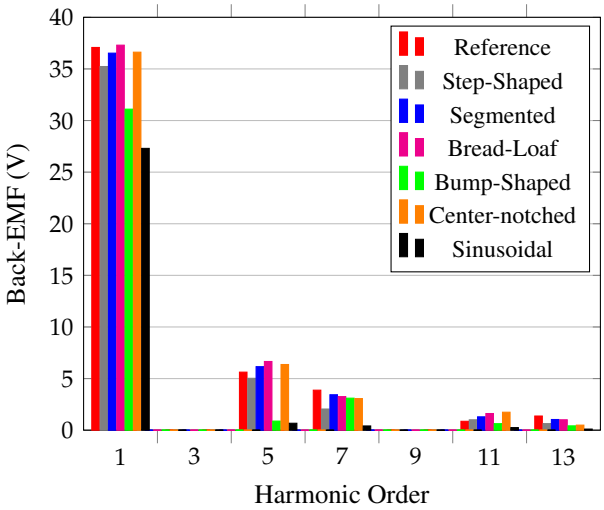

Figure 16. Back-EMF harmonic content amplitudes of all the design.

Table 2. Performance comparison of the proposed 1 kW motor with different rotor pole shapes.

Parameter	Unit	Radial Shaped Design	Step Shaped Design	Segmented Pole Design	Bread Loaf Shaped Design	Bump Shaped Design	Center Notched Design	Sinusoidal Shaped Design
Torque (T)	N·m	18.9	17.8	18.7	19.1	15.5	18.7	13.4
Cogging torque$_{(p-p)}$	N·m	9.66	4.87	5.07	2.43	1.15	2.93	0.67
Torque ripple	%	42.62	40.48	37.43	37.21	14.85	41.47	21.1
Peak flux-linkage	Wb	0.098	0.091	0.097	0.099	0.08	0.097	0.07
Flux-THD	%	4.88	3.82	5.29	4.67	4.18	5.36	10.09
Back-EMF THD	%	19.02	15.81	19.86	20.58	10.65	19.96	3.05
Power	kW	1	0.95	0.99	1.02	0.99	1	0.72
PM weight (W_{pm})	kg	0.805	0.748	0.792	0.723	0.648	0.794	0.536
T/W_{pm}	N·m/kg	23.478	23.796	23.611	26.417	23.919	23.551	25.000

4. Performance Comparison

The comparative performance analysis of a 1 kW, 510 rpm inner runner type RF-BLDC motor with lap winding and permanent magnet rotors of seven different shapes was carried out. Table 2 shows the performance comparison of all the designs. Compared to the reference design, the proposed step-shaped PM-RP design, segmented-pole design, bread-loaf shaped design, bump-shaped PM-RP design, center notched model, and sinusoidal-shaped design all exhibit reduced permanent magnet weight. It is also observed that the percentage torque ripple is reduced with all the proposed designs. Different performance parameters such as cogging torque, torque, output power, peak flux linkage, back-EMF THD, flux linkage THD and losses are also analyzed for all designs.

5. Conclusions

The design and comparative performance analysis of a three-phase, 1 kW, 510 rpm RF-BLDC motor with 24 -slots/8-poles combination were investigated. Different PM-RP shapes were proposed, analysed and compared with the reference configuration. The reference design has a radial PM-RP shape, while different proposed PM-RP shapes include step-shaped, segmented, bread loaf-shaped, bump-shaped, center notched, and sinusoidal-shaped. The electromagnetic performance of these proposed rotors was also investigated. The requirement for permanent magnet material is reduced in all the proposed rotor pole designs compared to the reference design. The minimum permanent magnet weight was observed in the sinusoidal-shaped rotor pole design. Compared with the reference design, a reduction in peak-to-peak cogging torque value was achieved by applying all the PM-RP shapes, i.e. 49.58% reduction with the step-shaped design, 47.51% with the segmented pole design, 74.84% with the bread-loaf-shaped design, and 69.66% by center-notched design. With the proposed bump-shaped design, an 88.09% reduction in peak-to-peak cogging torque was achieved, and the minimum cogging torque was achieved by the sinusoidal-shaped design. This study clearly shows that all the proposed techniques are efficient in reducing the cogging torque. However, each technique has its benefits and limitations. The proposed bump-shaped rotor pole showed the best results in torque ripple reduction and can be considered for other types of electric motors with different topologies.

Funding: This research received no external funding.

Author contributions: Conceptualization, T.J. and A.N.P.; Methodology, T.J. and A.N.P.; Software, T.J. and A.N.P.; Validation, T.J. and A.N.P.; Formal Analysis, T.J. and A.N.P.; Investigation, T.J. and A.N.P.;

Resources, T.J. and A.N.P.; Data Curation, T.J. and A.N.P.; Writing – Original Draft Preparation, T.J.; Writing – Review & Editing, T.J. and A.N.P.; Supervision, A.N.P.

Disclosure statement: The authors declare no conflict of interest.

References

[1] F. C. Mushid and D. G. Dorrell. Review of axial flux induction motor for automotive applications. In *2017 IEEE Workshop on Electrical Machines Design, Control and Diagnosis (WEMDCD)*, pages 146–151, 2017.

[2] Julio A. Sanguesa, Vicente Torres-Sanz, Piedad Garrido, Francisco J. Martinez, and Johann M. Marquez-Barja. A review on electric vehicles: Technologies and challenges. *Smart Cities*, 4(1):372–404, 2021.

[3] Ritvik Chattopadhyay, Md Sariful Islam, Ion Boldea, and Iqbal Husain. Fea characterization of bi-axial excitation machine for automotive traction applications. In *2021 IEEE International Electric Machines & Drives Conference (IEMDC)*, pages 1–7, 2021.

[4] Zhi Cao, Amin Mahmoudi, Solmaz Kahourzade, and Wen L. Soong. An overview of electric motors for electric vehicles. In *2021 31st Australasian Universities Power Engineering Conference (AUPEC)*, pages 1–6, 2021.

[5] Ramu Krishnan. *Permanent Magnet Synchronous and Brushless DC Motor Drives*. CRC Press, 1st edition, 2010.

[6] Deepak Mohanraj, Janaki Gopalakrishnan, Bharatiraja Chokkalingam, and Lucian Mihet-Popa. Critical aspects of electric motor drive controllers and mitigation of torque ripple—review. *IEEE Access*, 10:73635–73674, 2022.

[7] J. R. Miller, T. J. E.and Handershot Jr. *Design of Permanent Magnet Motor*. Oxford, Oxford University Press, U.K., 1994.

[8] D. C. Hanselman. *Brushless Permanent Magnet Motor Design*. McGrow-Hill, New York, 1994.

[9] Hongyun Jia, Ming Cheng, Wei Hua, Wenxiang Zhao, and Wenlong Li. Torque ripple suppression in flux-switching pm motor by harmonic current injection based on voltage space-vector modulation. *IEEE Transactions on Magnetics*, 46(6):1527–1530, 2010.

[10] T. Jhankal and A. N. Patel. Core edge inset radius variation technique to reduce cogging torque of interior permanent magnet synchronous motors. *International Journal of Scientific and Technology Research*, 9:6041–6048, 2020.

[11] Sang-Moon Hwang, Jae-Boo Eom, Geun-Bae Hwang, Weui-Bong Jeong, and Yoong-Ho Jung. Cogging torque and acoustic noise reduction in permanent magnet motors by teeth pairing. *IEEE Transactions on Magnetics*, 36(5):3144–3146, 2000.

[12] Haichao Feng, Sheng Zhang, Jinsong Wei, Xiaozhuo Xu, Caixia Gao, and Liwang Ai. Torque ripple reduction of brushless dc motor with convex arc-type permanent magnets based on robust optimization design. *IET Electric Power Applications*, 16(5):565–574, 2022.

[13] M. Aydin, Z. Q. Zhu, T. A. Lipo, and D. Howe. Minimization of cogging torque in axial-flux permanent-magnet machines: Design concepts. *IEEE Transactions on Magnetics*, 43(9):3614–3622, 2007.

[14] F. Caricchi, F.G. Capponi, F. Crescimbini, and L. Solero. Experimental study on reducing cogging torque and no-load power loss in axial-flux permanent-magnet machines with slotted winding. *IEEE Transactions on Industry Applications*, 40(4):1066–1075, 2004.

[15] Massimo Barcaro and Nicola Bianchi. Torque ripple reduction in fractional-slot interior pm machines optimizing the flux-barrier geometries. In *2012 XXth International Conference on Electrical Machines*, pages 1496–1502, 2012.

[16] N. Bianchi and S. Bolognani. Design techniques for reducing the cogging torque in surface-mounted pm motors. *IEEE Transactions on Industry Applications*, 38(5):1259–1265, 2002.

[17] Young-Hoon Jung, Myung-Seop Lim, Myung-Hwan Yoon, Jae-Sik Jeong, and Jung-Pyo Hong. Torque ripple reduction of ipmsm applying asymmetric rotor shape under certain load condition. *IEEE Transactions on Energy Conversion*, 33(1):333–340, 2018.

[18] Jingchen Liang, Amir Parsapour, Zhuo Yang, Carlos Caicedo-Narvaez, Mehdi Moallem, and Babak Fahimi. Optimization of air-gap profile in interior permanent-magnet synchronous motors for torque ripple mitigation. *IEEE Transactions on Transportation Electrification*, 5(1):118–125, 2019.

[19] Tanuj Jhankal and Amit N. Patel. Design and analysis of spoke type radial flux interior permanent magnet synchronous motor for high-speed application. In *2022 2nd Odisha International Conference on Electrical Power Engineering, Communication and Computing Technology (ODICON)*, pages 1–5, 2022.

[20] Li Zhu, S. Z. Jiang, Z. Q. Zhu, and C. C. Chan. Analytical methods for minimizing cogging torque in permanent-magnet machines. *IEEE Transactions on Magnetics*, 45(4):2023–2031, 2009.

[21] Xiuhe Wang, Yubo Yang, and Dajin Fu. Study of cogging torque in surface-mounted permanent magnet motors with energy method. *Journal of Magnetism and Magnetic Materials*, 267(1):80–85, 2003.

[22] Tanuj Jhankal and Amit N. Patel. Cogging torque minimization of high-speed spoke-type radial flux permanent magnet brushless dc motor using core bridge width variation technique. In *2023 International Conference on Recent Advances in Electrical, Electronics & Digital Healthcare Technologies (REEDCON)*, pages 750–755, 2023.

[23] Daohan Wang, Xiuhe Wang, Mun-Kyeom Kim, and Sang-Yong Jung. Integrated optimization of two design techniques for cogging torque reduction combined with analytical method by a simple gradient descent method. *IEEE Transactions on Magnetics*, 48(8):2265–2276, 2012.